DEFORMATION MECHANISMS IN Ti₃Al-Nb ALLOY AT ELEVATED TEMPERATURES

MEHANIZEM DEFORMACIJE V ZLITINI Ti₃Al-Nb PRI POVIŠANIH TEMPERATURAH

Srdjan Tadić[1], Radica Prokić-Cvetković[1], Igor Balać[1], Radmila Heinemann-Jančić[2], Katarina Bojić[1], Aleksandar Sedmak[1]

[1]Innovation Centre, Faculty of Mechanical Engineering, University of Belgrade, Serbia
[2] Faculty of Technology and Metallurgy, University of Belgrade, Serbia
srdjantadic26@gmail.com

Ti₃Al-11Nb-1V (*x*/%) was made in a vacuum arc furnace. Hot-rolling was conducted at 1050 °C in a two-phase field of the alloy. Strain-rate jump tests were performed at T = 800–1100 °C and strain rates of 10^{-6} to 10^{-3} s⁻¹. Creep stress exponent (n) and activation energy for deformation (Q) were used to identify deformation mechanisms. Two sequential mechanisms are revealed: (i) viscous glide, typical of solid solution alloys and, (ii) power law breakdown at lower temperatures. Activation energy for deformation was found to be strongly stress-dependant.

Keywords: Titanium intermetallics, deformation, viscous glide, power law breakdown

Zlitina Ti₃Al-11Nb-1V (*x*/%) je bila izdelana v vakuumski obločni peči. Vroče valjanje je bilo opravljeno pri 1050 °C v dvofaznem območju zlitine. Sunkoviti preizkusi hitrosti deformacije so bili narejeni pri T = 800–1100 °C in pri hitrosti deformacije 10^{-6} to 10^{-3} s⁻¹. Eksponent napetosti lezenja (n) in aktivacijska energija deformacije (Q) sta bila uporabljena za identifikacijo mehanizma deformacije. Odkrita sta bila dva sekvenčna mehanizma: (i) viskozno drsenje, ki je značilno za zlitine iz trdnih raztopin in (ii) prelom potenčnega zakona pri nižji temperaturi. Ugotovljeno je bilo, da je aktivacijska energija deformacije zelo odvisna od napetosti.

Ključne besede: titanova intermetalna zlitina, deformacija, viskozno drsenje, potenčni zakon, prelom zakona

1 INTRODUCTION

High-temperature mechanical properties and low density make the titanium aluminides attractive candidates for engine and airframe applications. Considerable efforts in research have been devoted to this class of materials, particularly to Ti₃Al-Nb alloy. This alloy consists typically of the ordered Ti₃Al α_2 phase (DO₁₉ structure, similar to h. c. p) and the b. c. c. β solution phase [1].

The main handicap of Ti₃Al-Nb alloys at room temperatures is attributed to limited ductility. It is ascribed due to the inadequate number of crystallographic slip systems [2]. However, at a higher temperature the alloy exhibits good ductility through thermal activated softening [3]. The high-temperature plasticity, thermomechanical processing and deformation mechanisms attracted the attention of a number of authors [4]. Three distinct high-temperature regimes of the thermomechanical processing were reported [5]: warm working (below 950 °C), hot working in the two phase field (980–1040 °C) and a hot working regime above the β-transus. In a more complex Ti-25Al-10Nb-3V-1Mo alloy, dynamic recovery and dynamic recrystallization were identified in the two-phase ($\alpha_2+\beta$) field [6]. It was suggested that the activation barrier for DRX in the ($\alpha_2+\beta$) field depends on the cross-slip in the α_2 phase [7]. Creep [8] and superplastic deformation [9] has also been well examined, although a lot of uncertainties remained. The identification of the rate controlling deformation mechanisms is still not fully clear in two phase alloys. Particularly confusing is the large scatter of activation energies [10,11] associated with deformation processes. Creep, transition to low-temperature creep and power law breakdown behaviour is the emphasis of this work. Deformation mechanisms are identified in terms of the creep stress exponent and activation energy for deformation.

2 EXPERIMENTAL

The alloy was prepared from a Ti-6Al-4V (with an extra low interstitials quality), high-purity aluminium and niobium flakes. It was smelted in a vacuum arc furnace under a low-pressure 'argon blanket'. Remelting was repeated several times in order to obtain a homogeneous, pore-free rod 20 mm in diameter. The nominal chemical composition of the alloy was as follows (by *x*/%): 24 % Al, 11 % Nb and 1 % V, Ti – the rest. After cleaning, the rod was hot-rolled on a laboratory two-high mill with ϕ-calibrated rolls, down to a diameter of 6 mm. Hot-rolling was conducted at 1050 °C in the two-phase field, well below the β-transus temperature. The rolling direction was swapped between two successive passes to eliminate the temperature gradient.

Compression test specimens with ϕ = 6 mm and 12 mm in height were machined from the previously chemically cleaned rod. The specimens were coated with fine molybdenum-sulfide powder to minimise barrelling. A series of strain-rate jump tests [12] were conducted on an "Instron" testing machine in a water-cooled vacuum chamber at temperatures ranging from 800 °C to 1100 °C. The temperature of the chamber was maintained within ±5 °C. The true strain rates were calculated [13] to be in the range from 10^{-6} to 10^{-3} s^{-1}. The tests were conducted down to 50 % of reduction of the specimen height. True stress was normalized with shear modulus μ = $5.1 \times 10^3 - 9T$ [14].

Metallographic specimens were prepared by wet grinding and diamond-paste polishing down to 1/4 μm. Keller's etchant was used to reveal the microstructure under the optical microscope.

3 RESULTS

The microstructure of the hot-rolled bar in a view normal to the rolling direction is shown in **Figure 1**. The microstructure consists of a homogeneously distributed α_2 phase in the β matrix. The average grain size of the α_2 phase is 17 μm.

The results of strain-rate jump test are summarized in **Figure 2**. It appears that stress follows a rather strong dependency on temperature and strain rate. For iso-structural tests, (T = const.), the stress sensitivity parameter, n, can be calculated as

$$n = \left(\frac{\partial \ln \varepsilon}{\partial \ln \sigma}\right) \tag{1}$$

The acquired data suggests that, according to Eq.1, the overall results might be separated into two fields: a low-stress regime with n = 3 (3.0 < n < 3.2) and an upper, high-stress regime, with n = 5 up to 9. Contrary to the low-stress field, where n is almost constant, in the high-stress region n gradually increases with temperature and stress. The boundary between low- and high-stress regions may be approximated using a straight line and
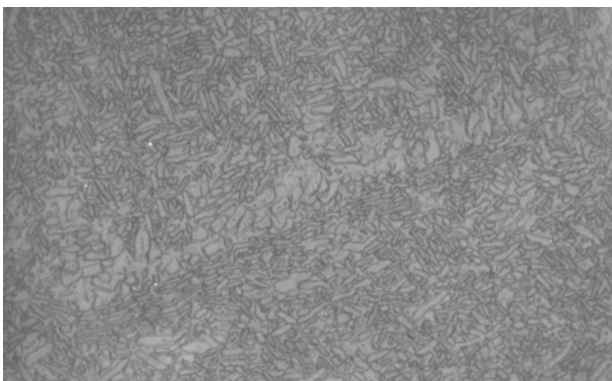

Figure 2: Strain-rates *vs.* normalized stress in the T = 1073–1373K range
Slika 2: Odvisnost hitrost deformacje – normalizirana napetost v območju T = 1073–1373 K

denotes, in fact, the transition between different deformation mechanisms.

The n = 3 value corresponds to alloy-type creep behaviour (Class A), the so-called viscous glide creep [15]. In contrast to this, metal-type creep behaviour (Class M) is recognized with n = 5 and usually points to a dislocation climb mechanism [16]. However, the stress-dependent gradual increase of n-values up to 9 suggests that power law breakdown (PLB) may be more probable [17].

The apparent activation energy for creep is given by,

$$Q_{app} = -R\left(\frac{\partial \ln \varepsilon}{\partial 1 / T}\right)_\sigma \tag{2}$$

where R is the gas constant. For constant stress values in the range of $\sigma/\mu = 4 \times 10^{-4} - 2 \times 10^{-3}$, the application of Eq. 2 is illustrated on **Figure 3**. Calculated activation

Figure 3: Activation energy for deformation. (Filled symbols – low stress regime in **Figure 2** hollow – high stress regime.)
Slika 3: Aktivacijska energija derformacije (polni znaki – režim majhne napetosti na **sliki 2**, prazni znaki – režim velike napetosti)

Figure 1: Microstructure of hot-rolled Ti₃Al-Nb alloy; (OM, x200)
Slika 1: Mikrostruktura vroče valjane zlitine Ti₃Al-Nb (OM, povečava 200-kratna)
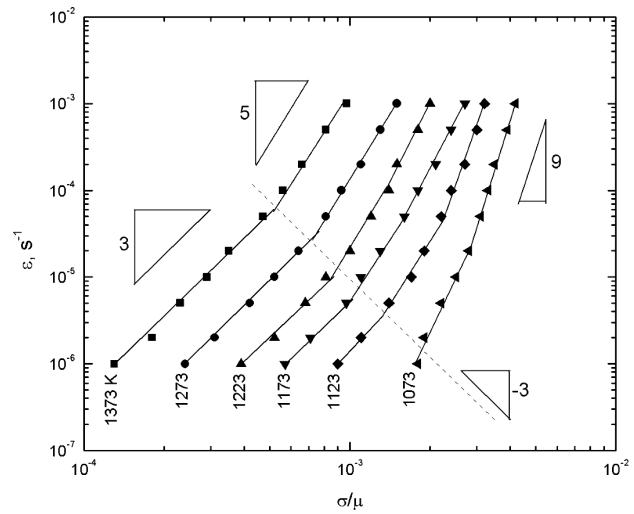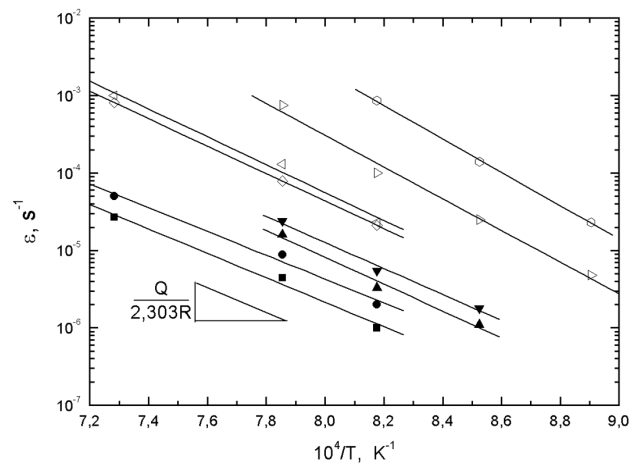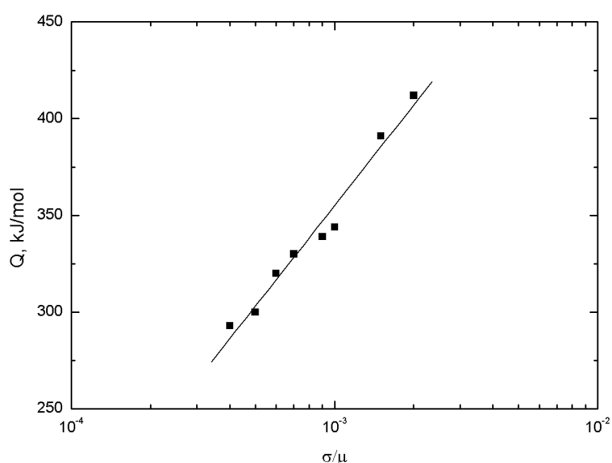
Figure 4: Semi-logarithmic stress- dependence of activation energies
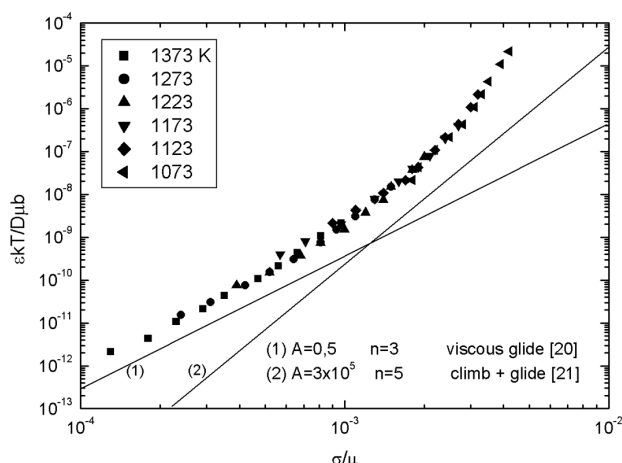**Slika 4:** Semilogaritmična odvisnost napetosti od aktivacijske energije

Figure 5: Diffusion-compensated strain rate as a function of normalized applied stress. Theoretical predictions of Eq. 3 are included.
Slika 5: Hitrost deformacije kompenzirana z difuzijo v odvisnosti od normalizirane delujoče napetosti. Vključene so teoretične napovedi iz enačbe. 3.

energies are shown in **Figure 4**. In the low-stress region, activation energies are within the range typical of lattice self-diffusion [10,11]. In the high-stress regime, Q values are higher and might be related to PLB [5]. Stress-dependent Q values require that, apart from the creep, dislocation glide mechanisms are operative. However, it is not yet clear which one is rate controlling.

Phenomenological relationship for power-law creep takes the well known form

$$\frac{\varepsilon kT}{D\mu b} = A\left(\frac{\sigma}{\mu}\right)^n \tag{3}$$

where A is a dimensionless constant, characteristic of that particular creep mechanism, D is the effective diffusion coefficient and all others have their usual meaning.

The effective diffusion coefficient is calculated using Eq. 4:

$$D = D_0 \exp\left(-Q/kT\right) \tag{4}$$

where Q represents the mean calculated activation energy and D_o is the so-called frequency factor. For the α_2 phase, $D_o = 2.24 \times 10^{-5}$ m²/s and for β,, $D_o = 3.53 \times 10^{-4}$ m²/s [18]. The effective diffusion coefficient is calculated to be within the range of $1.5 \times 10^{-20} - 5 \times 10^{-17}$ m²/s which is in good agreement with [18]. It should be pointed out that these values correspond to volume self-diffusion. For the viscous drag regime, appropriate diffusion would be Darken's chemical inter-diffusion and, for lower temperatures, pipe (core) diffusion is more likely to be operative [19]. Anyway, due to the lack of consistent published data, volume self-diffusion is used in further calculations. By applying Eqs. 3 and 4 to the experimental results, the plot of Figure 5 is revealed. Two segments are clearly distinguishable: (i) a linear one, with $n = 3$ and $A \cong 1$ up to the normalized stress in the vicinity of $\sigma/\mu = 10^{-3}$ and, beyond this stress, (ii) an exponential upward curve with continuous slope $n = 5$–9. Stress $\sigma/\mu = 10^{-3}$ at the departure of linearity is

widely accepted as a characteristic for PLB. **Figure 5** also includes theoretical calculations for viscous-glide [20] and climb-controlled creep [21]. Reasonable accord is more than clear, regardless of the diffusion approximations mentioned above.

It should be noted in **Figure 5** that $n = 5$ is only a small segment of the experimental data regarding higher stresses. This fact supports some confirmations that the behavior of $n = 5$ might be suppressed between viscous glide and power-law-breakdown [22,23]. In other words, with increasing stress (or lowering temperature), deformation advances sequentially: viscous-drag controlled glide → climb + glide controlled flow.

It is obvious that Eq. 3, due to PLB, cannot describe the overall deformation behaviour of the investigated alloy. For this reason, a more flexible, hyperbolic sine function is used:
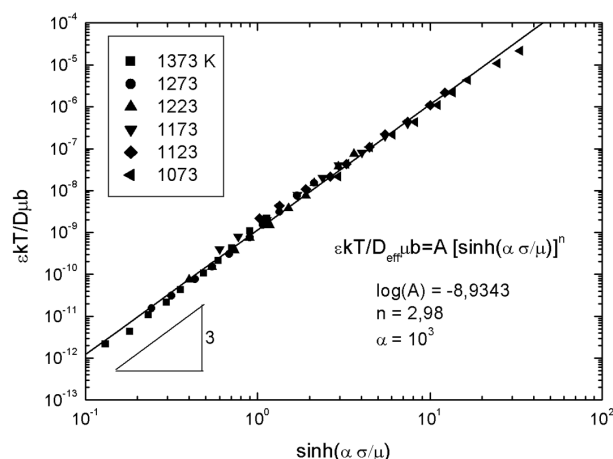

Figure 6: Hyperbolic sine fit (Eq. 5) of the data
Slika 6: Sinushiperbolični prikaz podatkov (enačbe 5)

$$\frac{\varepsilon k T}{D \mu b} = A \left[\sinh \left(\alpha \frac{\sigma}{\mu} \right) \right]^n \qquad (5)$$

Eq. 5 gives a good description of the creep and hot-working data, **Figure 6**. However, it is not the best possible linear fit. It has been searched for reasonable linear fit, yet parameters A, α and n reflect the physical meaning of deformation. In **Figure 6**, stress exponent $n \approx 3$ reflects viscous drag at low stresses; $\alpha = 10^3$ is the inverse of normalized stress for PLB, i.e. $\sinh(\alpha\sigma/\mu) = 1$ and, $A \approx 10^{-9}$ points to diffusion-normalized strain-rate for PLB. To repeat, some other values of A, α and n might yield better linearity of Eq. 5. However, it would be more valuable in technological modelling of hot-working), than from the academic merit of identification of deformation mechanisms.

4 DISCUSSION

Viscous glide has been reported to occur in a large number of solid solution alloys. In particular, aluminium alloys have been examined well [24–27]. Also, this phenomenon is observed commonly in a lot of intermetallics [28–31]. Two mutually competitive mechanisms are operative in this stress regime, dislocation glide and climb. Within the certain combination of materials' and technological parameters glide is the slower one and thus becomes the rate controlling mechanism of deformation.

Several possible viscous drag mechanisms were proposed. Cottrell and Jaswon [32] proposed that the dragging results from segregation of solute atmospheres to moving dislocations. The dislocation speed is limited by the rate of the solute atmosphere movement. Also, segregation to stacking faults is proposed [33]. Further, stress induced local ordering might be an obstacle to dislocation movement [34]. Finally, in long-range ordered alloys, as it is in the α_2 phase, dislocations are impeded due to anti-phase boundaries [35]. If only solute atmosphere dragging is considered, Mohamed and Langdon [24] proposed the relationship for creep in viscous glide:

$$\varepsilon = \frac{\pi(1-\nu)kTD}{6e^2 cb^5 \mu} \left(\frac{\sigma}{\mu} \right)^3 \qquad (6)$$

where e is the solute-solvent size difference, c is the concentration of solute atoms and D is the chemical diffusion coefficient for the solute atoms. Eq. 6 serves as an explanation that viscous glide occurs preferably in materials with a relatively large atom size mismatch (e) and higher solute concentrations (c). InTi₃Al-Nb alloy, both aluminium and niobium atoms act as solutes in the β-phase solid solution. In the α_2 phase niobium may substitute both Ti and Al atoms. The atomic volumes of Ti and Nb are almost identical. However, the atomic diameter of an Al atom is much lower than that of a titanium atom [19]. Also, viscous glide seems to be particularly strong at high temperatures where the volume fraction of the β-phase (Vf_β) dominates over α_2. For

example, from the quasi-binary phase diagram Ti₃Al-Nb [36], it can be calculated that Vf_β at $T = 1373$ K is 90 %, at $T = 1273$ K $Vf_\beta = 65$ % while at $T = 1073$ K β is only 30 %. This suggests strongly that the aluminium-rich β-phase is predominantly in charge of viscous glide.

The transition from viscous glide to climb controlled creep has been the subject of numerous investigations [37–41]. There is a general agreement that the transition is due to the breakaway of dislocations from solute atmospheres. Under some critical stress the glide becomes faster than the climb and the latter starts to be the rate controlling mechanism. The break-away stress is proposed [42]:

$$\sigma = \left(\frac{W_m^2}{2^{\beta-1} kTb^3} \right) c \qquad (7)$$

W_m is the maximum interaction energy between a, solute atoms and dislocations, c is the solute concentration and β is the factor which depends on the nature of the impurity clouds. Interaction energy W_m is

$$W_m = -\frac{1}{2\pi} \left(\frac{1+\nu}{1-\nu} \right) \mu |\Delta V_a| \qquad (8)$$

Where ν is Poisson's ratio ($\nu = 0.24$), μ is shear modulus (Eq.1) and ΔV_a is volume difference between solute and solvent atoms. From [19], $V_{Al} = 1.66 \times 10^{-29}$ m³ and $V_{Ti} = 1.81 \times 10^{-29}$ m³, and $\Delta V_a = 0.15 \times 10^{-29}$ m³. With $b = 2.83 \times 10^{-10}$ m, and the atomic concentration of aluminium $c_{Al} = 0.25$, Eqs. 8 and 7 give good agreement within the order of magnitude with the experimentally determined $\sigma/\mu \approx 10^{-3}$. However, there is no doubt that interstitial impurities sustain break-away stress strongly.

While the viscous glide regime is clearly distinguishable, the distinction between five-power-law and PLB isn't so obvious. Close inspection of **Figure 2, 5, and 6** suggests strongly that the $n = 5$, regime is not particularly a defined creep regime of this alloy, but presents only the very beginning of PLB. Suppression of five-power-law between viscous glide and PLB is also found in some Al-Mg [43] and Al-Zn alloys [44].

Typically, within PLB, as n increases activation energy decreases. However, in this work, a conflicting result was found – activation energy is somewhat higher as n increases. The behaviour of the Q values in Figure 4 excludes inaccurate scatter of data. Such a result might be rationalized trough the fact that the ductile β-phase and more rigid α_2-phase may behave quite differently during deformation. Eq. 2, used to calculate activation energy, is derived from

$$\varepsilon = A\sigma^n \exp\left(-\frac{Q}{RT} \right) \qquad (9)$$

If multiple deformation processes occurs through sequential serial steps, (as glide and climb are), activation energy corresponds to the slowest one. However, if parallel, simultaneous mechanisms are operative, activation energy corresponds to the fastest one. Assum-

ing that applied stress is equally distributed on both phases, the so-called iso-stress model [45] results in:

$$\sigma = \sigma_{\alpha_2} = \sigma_\beta \Rightarrow \varepsilon = \varepsilon_{\alpha_2} V_{\alpha_2} + \varepsilon_\beta V_\beta \quad (10)$$

meaning that the strain-rates of phases might depend strongly on volume fractions (V). Combining Eqs 9, 10 yields

$$\varepsilon = A_{\alpha_2} \sigma^{n_{\alpha_2}} V_{\alpha_2} \exp\left(-\frac{Q_{\alpha_2}}{RT}\right) + A_\beta \sigma^{n_\beta} V_\beta \exp\left(-\frac{Q_\beta}{RT}\right) \quad (11)$$

A similar result can be obtained from a so-called iso-strain-rate model [46] ($\varepsilon = \varepsilon_{\alpha_2} = \varepsilon_\beta$). The main conclusion from Eq.11 (and similar two-phase deformation models [47–50]), is that simultaneous mechanisms may be operative in the α_2 and β phases during deformation. In that case, apparent activation energy might be reflected by the 'faster' phase. The same issue might be seen in **Figure 5**, where experimental results follow the faster of the two theoretical mechanisms.

5 CONCLUSIONS

Strain-rate-jump tests were performed on two-phase Ti₃Al-Nb alloy in a wide range of temperatures (1073–1373 K) and strain rates from (10^{-6} to 10^{-3} s^{-1}). Deformation mechanisms were identified in terms of stress-exponent (n), activation energy (Q) and fitting with known theoretical equations.

1. Viscous glide ($n = 3$ and Q close to lattice self diffusion) was identified at a high temperature, low-stress regime.
2. The five power law is suppressed between the viscous glide and power law breakdown.
3. Power law breakdown begins at $\sigma/\mu \approx 10^{-3}$, very common in most metals and alloys, and features a continuous, stress dependent, increase of n and Q.
4. Deformation behaviour of the alloy can be well described with hyperbolic sine function.

6 REFERENCES

[1] Koss D A, Banerjee D, Lukasak D A, Gogia A K, In *High temperature aluminides and intermetallics,* (eds.) S H Whang, C T Liu, D P Pope, J O Steigler (Warrendale, PA: The Mater. Soc.), (1990), p.175

[2] Nandy T K, Banerjee D, In *Structural intermetallics* (eds.) M V Nathal, R Darolia, C T Liu, P L Martin, D B Miracle, D B Miracle, R Wagner, M Yamaguchi (Warrendale, PA: The Mater. Soc.), (1997), p.777

[3] C. Huang, T. A. Loretto, *Mater.Sci.Eng. A19* (**1995**), 39

[4] Banerjee D, Gogia A K, Nandy T K, Muraleedharan K, Mishra R S, In *Structural intermetallics,* (eds) R Darolia, J J Lewandowski, C T Liu, P L Martin, D B Miracle, M V Nathal (Warrendale, PA: The Mater. Soc.), (1993), p.19

[5] S. L Semiatin, K. A. Lark, D. R. Barker: *Met. Trans.* 23A (**1992**), 295

[6] M. Long, H. J. Rack: *Mater.Sci.Eng.* A170 (**1993**), 215

[7] P. K. Sagar, Y. Prasad: *Z.Metallkd.* 89 (**1998**) 6, 433

[8] P. K. Sagar, D. Banerjee, Y. Prasad: *Met. Trans.* 27A (**1996**), 259

[9] J. W. Zhang, C. S. Lee, D. X. Zou, S. Q. Li, J. K. Lai, *Met.Trans.A,* 29A (**1998**), 559

[10] H. S. Yang, P. Jin, E. Dalder, A. K. Mukherjee, *Scr.Met.Mater.,* 24 (**1990**), 1319

[11] H. C. Fu, J. C. Huang, T. D. Wang, C. C. Bampton, *Acta Mater.,* 46 (**1998**), 465

[12] J. P. Pilling, N. Ridley, Superplasticity in Crystaline Solids, The Institute of Metals, (1989), London

[13] G. E. Dieter, *Mechanical Metallurgy*, McGraw-Hill, (1988), London

[14] J. C. Huang, H. C. Fu, B. Y. Lou, H. L. Lee, *Scr.Mat.,* 39 (**1998**), 95

[15] T. G. Langdon, In *2nd Riso International Symposum on Metallurgy and Materials Science*, (Eds) N. Hansen, A. Horsewell, T. Leffers, H. Lilholt, (1981), Riso Nat.Lab

[16] M. E. Kassnera, M. T. Perez-Prado, *Prog. in Mat. Sci.* 45 (**2000**), 1–102

[17] S. V. Raj, A. D. Freed, In *Unified Constitutive Laws of Plastic Deformation*, (eds) A. S. Krausz, K. Krausz, Academic Press, 1996

[18] Y. Mishin, C. Herzig, *Acta mater.* 48 (**2000**), 589

[19] H. Frost, M. F. Ashby: *The plasticity and creep of metals and ceramics*, Pergamon Press, Oxford (1982), 175 p.

[20] J. Weertman, Trans ASM, 61 (**1968**), 681

[21] J. E. Bird, A. K. Mukherjee, J. E. Dorn, *Quant.Relation Between Properties and Microstructure*, Israel University Press, (1969), Jerusalem

[22] H. Oikawa, K. Honda, S. Ito, *Mater Sci Eng* (**1984**), 64

[23] M. S. Soliman, F. A. Mohamed., *Metall Trans A*, (**1984**), 15

[24] F. A. Mohamed, T. G. Langdon, *Acta Metall*, 22 (**1974**), 779

[25] K. L. Murty, F. A. Mohamed, J. E. Dorn, *Acta Metall*, 20 (**1972**), 1009

[26] W. R. Cannon, O. D. Sherby, *Metall Trans*, (**1970**), 1030

[27] P. K. Chaudhury, F. A. Mohamed, *Mater Sci Eng A* (**1988**), 101

[28] T. G. Nieh, W. C. Oliver, *Scripta Metall*, 23 (**1989**), 851

[29] J. Wolfenstine, *J Mater Sci Lett*, 9 (**1990**), 1091

[30] D. Lin, A. Shan, D. Li, *Scripta Metall Mater*, 31 (**1994**), 1455

[31] D. Li, A. Shan, Y. Liu, D. Lin, *Scripta Metall Mater*, 33 (**1995**), 681

[32] A. H. Cottrell, M. A. Jaswon, *Proc Roy Soc London A,* 199 (**1949**), 104

[33] J. C. Fisher, *Acta Metall*, 2 (**1954**), 9

[34] H. Suzuki, *Sci Rep Res Inst Tohoku University A*, 4 (**1957**), 455

[35] G. Shoeck, In *Mechanical behavior of materials at elevated temperature*, (ed. J. E. Dorn, New York, McGraw-Hill, 1961

[36] A. K. Gogia, R. G. Baligidad, D. Banerjee, *Sadhana* 28, (**2003**) 3&4, 677

[37] P. Yavari, T. G. Langdon, *Acta Metall*, 30 (**1982**), 2181

[38] K. L. Murty, *Scripta Metall*, 7 (**1973**), 899

[39] K. L. Murty, *Phil Mag*, 29 (**1974**), 429

[40] A. Orlova, J. Cadek , *Z Metall*, 65 (**1974**), 200

[41] F. A. Mohamed, *Mater Sci Eng*, 38 (**1979**), 73

[42] J. Friedel, *Dislocations,* Oxford, Pergamon Press, (1964)

[43] H. Oikawa, K. Honda, S. Ito, *Mater Sci Eng*, 64 (**1984**), 237

[44] M. S. Soliman, *J. of Mat.Sci.*, 22 (**1987**), 3529

[45] T. H. Courtney, *Mechanical Behavior of Materials*, McGraw-Hill, (1990), New York

[46] K. Cho, J. Gurland, *Metall Trans A*, 19A (**1988**), 2207

[47] S. Ankem, H. Margolin, *Metall Trans*, 17A (**1986**), 2209–26

[48] D. Kolluru, T. Pollock, *Acta Mater*, 46 (**1998**), 2859

[49] V. Hasija, S. Ghosh, M. Mills, D. Joseph D, *Acta Mater*, 51 (**2003**), 4533

[50] M. H. Yoo, S. R. Agnew, J. R. Morris, K. M. Ho, *Mater Sci Eng A,* 319 (**2001**), 87